NASA Technical Memorandum 88289

Flight Test Techniques for the X-29A Aircraft

John W. Hicks, James M. Cooper, Jr., and Walter J. Sefic

February 1987

National Aeronautics and
Space Administration

NASA Technical Memorandum 88289

Flight Test Techniques for the X-29A Aircraft

John W. Hicks, James M. Cooper, Jr., and Walter J. Sefic
Ames Research Center, Dryden Flight Research Facility, Edwards, California

1987

NASA
National Aeronautics and
Space Administration
Ames Research Center
Dryden Flight Research Facility
Edwards, California 93523-5000

FLIGHT TEST TECHNIQUES FOR THE X-29A AIRCRAFT

John W. Hicks,* James M. Cooper, Jr.,** and Walter J. Sefic†

NASA Ames Research Center
Dryden Flight Research Facility
Edwards, California

Abstract

The X-29A advanced technology demonstrator is a single-seat, single-engine aircraft with a forward-swept wing. The aircraft incorporates many advanced technologies being considered for this country's next generation of aircraft. This unusual aircraft configuration, which had never been flown before, required a precise approach to flight envelope expansion. Special concerns were static wing divergence and a highly unstable airframe. Flight envelope expansion included the 1-g flight envelope and the maneuver envelope at higher normal load factors and angle of attack. Real-time analysis was required to clear the envelope in a safe, efficient manner. In some cases, this led to development of a unique real-time analysis capability. The use of real-time displays to provide for quick analysis of stability and control, dynamic and static structures, flight control systems, and other systems data greatly enhanced the productivity and safety of the flight test program.

This paper describes the real-time analysis methods and flight test techniques used during the envelope expansion of the X-29A aircraft, including new and innovative techniques that provided for a safe, efficient envelope expansion. The use of integrated test blocks in the expansion program and in the overall flight test approach will be discussed.

Nomenclature

ACC	automatic camber control
AR	analog reversion
BFF	body-freedom flutter
DR	digital reversion
FCS	flight control system
FDMS	flight deflection measurement system
FM	frequency modulation
FSW	forward-swept wing
g	normal load factor
ITB	integrated test block
LED	light-emitting diode
MCC	manual camber control
PCM	pulse-code modulation
pEst	parameter estimation program
RAV	remotely augmented vehicle

Introduction

The unique X-29A forward-swept-wing aircraft required a specially tailored flight test program to efficiently, yet safely, expand the 1-g and maneuver envelopes while gathering research data to evaluate several highly integrated advanced technologies. Conducting a multidisciplinary test program on a single experimental aircraft of radical design was very challenging. The program required tightly coordinated flight test planning coupled with specially developed maneuver techniques and real-time and postflight data analysis capabilities. Heavy reliance on ground and in-flight simulation and extensive predictive preflight analysis were also essential to program success. Several specific technical areas, such as classical flutter, aeroservoelasticity, flight control system (FCS) stability, structural loads, aircraft systems, propulsion, performance, and basic stability and control characteristics, had to be cleared on a single airplane. A flight rate of up to four flights per day (high for an X-type airplane) and two flight days per week required an emphasis on real-time analysis. Specialized real-time analysis techniques had to be developed to get critical answers while in flight to clear the aircraft to the next envelope point.

The X-29A project was begun in 1977 by the Defense Advanced Research Projects Agency (DARPA) and the Grumman Aerospace Corporation. Because of the obvious safety-of-flight advantages of the Edwards Air Force Base complex, the decision was made to ship the aircraft to Edwards AFB for its first flight and conduct the entire envelope expansion program there. It was shipped through the Panama Canal, arriving at Edwards AFB in October 1984. A flight test team, located at the NASA Ames Research Center's Dryden Flight Research Facility (Ames-Dryden) and made up of Ames-Dryden, Air Force Flight Test Center, and Grumman personnel, successfully completed the first flight on December 14, 1984. Ames-Dryden was the responsible test organization, with safety-of-flight and operational responsibility. (Further details of programmatic issues can be found in Ref. 1.) The flight envelope expansion was completed by the end of 1986. The prime objective was the expansion of the 1-g flight envelope in Mach number and altitude and the angle of attack and normal load factor maneuvering envelope to the limits determined by the FCS and structural ground tests.

With the restriction of a single airplane, several technical discipline test requirements and envelope clearance tasks had to be integrated into the flight program. These included controls, structural loads, structural dynamics, aircraft systems, and propulsion. More research-oriented

*Chief Engineer, X-29 Program. AIAA member.
**Aerospace Engineer.
†Project Manager, X-29 Program. AIAA member.

investigations of aircraft performance, local aerodynamics, handling qualities, and stability and control derivative extraction were also included. Structural loads had to clear both the basic airframe loads envelope in the automatic camber control (ACC) wing configuration mode and the static wing divergence in manual camber control (MCC) mode.

Aircraft Description

The X-29A advanced technology demonstrator (Fig. 1) is a single-seat aircraft designed to evaluate the synergistic effects of several integrated technologies to advance the state of the art of this country's next generation of fighter aircraft. Its most notable feature is the forward-swept wing (FSW) having a 33.73° quarter-chord wing sweep. The primary wingbox is covered with aeroelastically tailored graphite epoxy covers attached to conventional aluminum and titanium spars. The load-bearing wing covers give a lightweight, yet strong, structure that controls wing deflection and the tendency of the FSW toward wing divergence. The wing has a 5-percent-thick supercritical airfoil, a fixed leading edge, and full-span, dual-hinged trailing flaperons, which yield high lift during takeoff and landing and provide the sole source of lateral control for the aircraft. The flap is also used to vary the wing camber either automatically with the continuous ACC mode or manually by the pilot using the discrete MCC mode. Flaperon deflection range is from 10° trailing edge up to 25° trailing edge down. The wing aerodynamics are coupled with a full-authority, high-rate canard located forward of the wings at the leading edge of the engine inlets. The travel of the canards is 30° leading edge up to 60° leading edge down at a maximum rate of 100 deg/sec. Aft-mounted fuselage strake flaps with a ±30° travel work in conjunction with the canards and symmetrically deflected flaperons to provide a unique three-surface aircraft pitch control. A single-piece rudder provides yaw control. The aircraft forward of the engine inlets consists of a standard F-5A nose section, cockpit, and nose gear.

The nominally 35-percent negative static margin of the aircraft is stabilized by a highly augmented triplex digital-analog fly-by-wire control system. The FCS has three modes: normal (primary) mode, digital reversion (DR) mode, and analog reversion (AR) mode.

Propulsion is provided by a single General Electric F404-GE-400 afterburning engine, rated at 16,000 lb thrust at sea level. The engine is mounted in a fuselage with two side-mounted, fixed-geometry inlets that were designed for transonic performance. Aircraft takeoff gross weight is 17,800 lb with a 4000-lb fuel capacity in the fuselage and strake tanks.

Instrumentation

The flight test instrumentation system (Fig. 2) was tailored for envelope expansion and some flight research measurements. Because of airframe internal volume constraints, a 10-bit remote unit pulse-code modulation (PCM) system was used for data aquisition. The outputs of the five PCM units and the ARINC 429 (Aeronautical Radio, Incorporated) data bus are combined in an instrumentation component known as an interleaver and are output as a serial PCM stream. In addition, a constant-bandwidth frequency modulation (FM) system is installed to acquire high-response acceleration and vibration data. The output of the FM mutiplexer is routed to a premodulation mixer where it is combined with the pilot's voice. Air-to-ground telemetry is the only source of aircraft data since there is no onboard recording system. Instrumentation provisions include measurements for structural loads and dynamics, flight controls, stability and control, aircraft subsystems, propulsion, and performance. The F404-GE-400 engine contains an F-18-style flight test thrust instrumentation system, but only the GE basic engine instrumentation portion was put into operation for the envelope expansion phase. More discussion of engine instrumentation can be found in Ref. 2.

Externally, 12 infrared light-emitting diodes (LEDs) were mounted across the top of the right wing as part of the flight deflection measurement system (FDMS). The LEDs transmitted light to a dual receiver mounted in the right side of the fuselage above the wingroot. The left wing, canard, strake, and strake flap upper surfaces were instrumented with 179 flush-mounted static pressure taps to measure aerodynamic pressure distribution. Finally, each wing pontoon, containing the mid- and outboard flaperon hydraulic actuator, was fitted with a special aft-mounted flaperon eccentric-rotary-mass structural excitation system to investigate the supersonic flap-tab single-degree-of-freedom flutter potential. The FDMS and structural excitation system are temporary external devices used specifically to assist in the structural clearance of the flight envelope.

Real-Time Processing and Display

The NASA Ames-Dryden Western Aeronautical Test Range provided the real-time monitoring and analysis capability for the envelope expansion work. Since all data from the X-29A aircraft were available only over a telemetry downlink during flight, all data had to be recorded, and in some cases analyzed, in real time on the ground. The telemetry downlink and data processing setup is outlined in Fig. 3. The range provides telemetry acquisition and processing, real-time data analysis and display, voice communication links, radar tracking for space positioning, and video displays of the aircraft in flight. This information was made available to two mission control rooms, the "blue room" and the spectral analysis facility, which worked in parallel to direct the flights. The blue room consists of 12 strip charts, numerous CRT displays, and a terminal console hookup to a computer providing real-time data processing. Gould SEL 32/55 and 32/77 minicomputers are used to process telemetry information, to calibrate it, to convert it to engineering units, and to display it to the control room. This control room contains the test conductor, range communications personnel, project management, and discipline engineers from controls, propulsion, systems, loads, and aerodynamic stability and control.

The spectral analysis facility consists of six strip charts, CRT displays, a communications

link to the blue room, and two real-time computers. One of the computers, an HP 5451C Fourier Analyzer, is used to extract structural dynamics frequency and damping data for the primary airframe modes. The second computer, a Gould Concept Series 9780, is used at a flight controls station to analyze controls system frequency response to determine system stability margins. Reference 3 contains a more complete description of the NASA Ames-Dryden range facilities.

Basic Flight Test Approach

Several technical areas of concern had an impact on the basic X-29A flight envelope clearance. The primary objective, of course, was to clear the aircraft in speed and altitude and in angle of attack. Another goal was to attain some level of positive normal load factor capability on the aircraft, not only to obtain loads data but also to be able to maneuver the aircraft at a given Mach number and altitude. Minimum stability margins of the aircraft FCS had to be maintained throughout the flight envelope and were a concern in the transonic flight regime. The actual FCS stability trends for such a highly unstable airplane were uncertain. Structural static wing divergence and the coupling of the pitch short-period mode with the first wing bending mode (this coupling is known as body-freedom flutter) were strong influences on the envelope expansion approach as dynamic pressure increased. Canard loading effects in the transonic area at high dynamic pressures also had a strong influence. A possible supersonic flutter mode in the dual-hinged wing-mounted flaperons was another concern; the flaperon rotary-mass shaker system was used in an attempt to identify this phenomenon. Overall, aircraft aerodynamic stability and control surface effectiveness, especially transonically and at higher angles of attack, affected the approach to parameter estimation of the aerodynamic derivatives.

The basic approach used in expanding the X-29A flight envelope was to first clear the 1-g flight envelope at a given Mach number and altitude. The second step was to fly at the next lower Mach number at that given altitude and clear the maneuver envelope in angle of attack and normal load factor. Typically, Mach number increments for envelope expansion were 0.05 subsonically, 0.02 transonically, and 0.1 supersonically. Figure 4 shows the 1-g flight envelope test point matrix and a typical sequence (solid symbols) used to clear the envelope. Primarily because of structural clearance considerations, a specific dynamic pressure level was first approached at a higher altitude, which allowed for a more gradual increase in dynamic pressure with Mach number than at a lower altitude. The expansion then continued at a constant dynamic pressure by flying to the corresponding Mach number at the next lower target altitude, usually 10,000 ft below the previous one. This was followed until the low-altitude, high-Mach-number region was reached, where constant-altitude expansion was substituted for constant dynamic pressure due to considerations of static wing divergence clearance. In addition to the test maneuvers designed to expand the flight envelope, the angle-of-attack and normal load factor expansion maneuver sequence contained some added maneuvers. These maneuvers were designed to obtain special flight research data to aid in evaluating the advanced technologies. The actual envelope expansion took place in two phases. The first phase was the limited flight envelope expansion below Mach 0.60 and 30,000 ft. After checking out the aircraft in this region and making some FCS modifications, the rest of the full 1-g envelope was expanded to 40,000 ft and supersonically to maximum speed.

Integrated Test Block Approach

The 1-g envelope clearance was accomplished by performing a series of maneuvers at a given altitude and Mach number. Two integrated test blocks (ITBs) were developed to clear the aircraft envelope in several discipline areas. The ITB-1 was used for the 1-g envelope clearance and consisted of the following four maneuvers:

1. Structural dynamics block
   - 1-min stabilized point
   - Three-axis control raps
   - 15-sec hands-off trim point

   This block was used to clear the aeroservoelastic and flutter envelopes. The three-axis raps and natural turbulence excitation put energy into the structure. The hands-off point was used to accomplish airspeed and angle-of-attack calibrations.

2. Longitudinal block
   - Fast-slow pitch doublet
   - Repeat doublet
   - Stick rap
   - Frequency sweep

   This block was used to gather data that were entered into the real-time phase and gain margin controls clearance routines. Approximately 15 sec after completion of this block, a clearance could be passed to the pilot. This block was also used to gather data for the longitudinal stability and control analysis that generated aerodynamic derivatives in postflight processing and to clear the 1-g static loads envelope.

3. Lateral block
   - Roll-yaw doublet
   - Repeat doublet
   - Full-stick 0° to 60° rolls, left and right
   - Stick rap
   - Frequency sweep

   This block was used to gather lateral-directional stability and control derivatives. The frequency sweep was used to generate lateral-directional handling qualities parameters.

4. Directional block
   - Yaw-roll doublet
   - Pedal rap

   This block was used to gather data for static loads and stability and control clearance.

With the successful completion of the ITB-1 at any given Mach number, the aircraft was slowed, usually by 0.05 Mach number, and a maneuver clearance block, ITB-2, was performed. This block

expanded the angle-of-attack, normal load factor, and maneuver capabilities of the vehicle by including the following maneuvers:

1. Steady-heading sideslips
   3° sideslip
   Full-pedal or limit sideslip

These were used to gather static loads and lateral-directional stability and control data.

2. Roll-yaw doublets at half-maximum sideslip

3. Full-stick 0° to 60° rolls, left and right

These rolls were used to gather loads, controls, and handling qualities data. These were buildup maneuvers to the 360° roll.

4. Full-stick 360° roll, left and right

These rolls were used to gather loads, controls, and handling qualities data.

5. Roll-pitch step inputs

These 0.5-in step inputs and the resultant control and aircraft responses were used for simulation correlation work.

6. Constant-altitude windup turn

Data from these maneuvers were used in the loads, controls, and wing pressure disciplines for load clearance. These maneuvers were accomplished to the cleared loads envelope to establish data that would allow further load clearance.

7. Constant-thrust windup turns

Data from these turns were used in the performance discipline to derive drag polars.

8. Pushover-pullups

This wings-level sequence consisted of 1-g stabilized flight, a pushover to 0 g followed by a pullup to 2 g, and a return to 1-g stabilized flight. These maneuvers were used to develop drag polar shapes and to fill in the 0- to 1-g loads range.

The ITB-1 and ITB-2 maneuvers cleared the ACC flight control mode. The MCC flight control mode was then evaluated by a full ITB-1 followed by pushover-pullups and windup turns. These data were used primarily in wing divergence analysis to establish the static wing divergence dynamic pressure predictions.

By using the integrated test block approach, the X-29A aircraft was taken through the flight envelope while simultaneously clearing areas of concern in various disciplines.

Having cleared the 1-g and maneuvering envelopes, the emphasis shifted to gathering research data. Numerous maneuver blocks were set up for the different disciplines. For example, the loads research group established the following set of maneuvers to build up their X-29A data base:

1. Symmetric pullup
2. Symmetric pushover
3. Left and right turn reversal
4. Left and right rudder kick
5. Left and right rudder reversal

Structural Dynamics Techniques

The primary real-time analysis technique used to track the structural frequency and damping of five main modes was the random-data auto-power-spectrum analysis. The five modes included the first symmetric and antisymmetric wing bending modes, the first fuselage vertical and lateral bending modes, and the first vertical fin bending mode. Monitoring the symmetric first wing bending modal frequency in real time was especially important in tracking the onset of the body-freedom flutter (BFF) phenomenon. While actual mode coupling occurs at about 2 Hz, onset was predicted to begin as early as 5 Hz. The BFF phenomenon acts as a precursor to the static wing divergence problem. At a given Mach number and altitude condition, data from an approximately 60-sec interval were required for analysis. The required maneuver consisted of a stabilized point with random air turbulence and three-axis stick rap inputs. The eccentric rotary-mass flaperon excitation system was also used at times as an input for the entire airframe. The primary function of the flaperon excitation system, however, was to provide wing excitation to track the supersonic flap-tab single-degree-of-freedom flutter.

A fast Fourier analysis was performed on the data with a minicomputer using a frame size of 1024 data samples at 100 samples/sec. On the ground, an analog bandpass filter was used to isolate each structural mode. In a similar manner, postflight analysis of the same maneuver points was performed on the canard random data using a frame size of 2048 samples at 200 samples/sec. The inverse Fourier transform was computed to obtain the autocorrelation function from which a data cutoff time could be selected and smoothing performed to obtain a smoothed auto-power-spectrum display (Fig. 5). Each mode in the auto-power-spectrum display was fit with a least-squared-error parabolic curve whose modal frequency was the maximum amplitude of the curve, and the damping was extracted using the half-power technique. More specific information on the method can be found in Ref. 4. The actual frequency and damping of the five main modes were compared in real time with precomputed predictions (Fig. 6). Damping or modal frequency that were significantly lower than predictions caused a halt in the envelope expansion until the problem was understood.

Stability and Control

Aircraft aerodynamic characteristics were analyzed by extracting the nondimensionalized aerodynamics derivatives, using an interactive parameter estimation program known as pEst. Special three-axis stick doublet maneuvers were used as data input to the computer program. To increase the information content of the data, these maneuvers consisted of pairs of fast and slow doublets in each axis, which were repeated

for the longitudinal and lateral cases. The highly augmented three-surface integrated pitch control made the extraction of the three separate control surface derivatives impossible during the envelope expansion phase of the program. For this reason, only an effective pitch control power derivative could be extracted, representing the combined pitch control of all three surfaces. The Cramér-Rao bound was applied to determine the uncertainty levels in the individual derivatives, and the data scatter was used to determine the validity of the derivatives.

The high longitudinal static instability of the X-29A aircraft requires artificial stabilization by the high-response FCS. As a result, the aircraft response is dominated by the FCS rather than by aerodynamics. Safety-of-flight considerations and the dominance of the FCS necessitated the development of a real-time analysis technique to monitor the longitudinal-axis control system stability. A fast Fourier transform technique was used to measure open-loop frequency response and the corresponding phase margin at the gain crossover frequency and gain margins at the high and low phase crossover frequencies. Real-time calculations were compared with preflight computed predictions as the envelope expanded from point to point in Mach number and altitude. The stability criterion used to halt envelope expansion to the next Mach number point was a minimum gain margin of 3 dB or a phase margin of 22.5°, or both, based on MILSPEC-F-9490D (Ref. 5). Significant adverse trends toward those minimums also slowed or halted the envelope expansion process until the situation was understood and a remedy was developed. This real-time capability was of great value to the program. Using postflight analysis, only one expansion point could have been flown per flight and only one flight every two to three days. The real-time implementation of the stability margin analysis and real-time clearance of the FCS performance allowed the clearance of two or three Mach number and altitude points per flight at up to four flights per day. This greatly accelerated the envelope expansion phase.

The real-time open-loop frequency response analysis required about 52 sec of flight data recorded at 40 samples/sec, or a total of 2048 time history data points. The maneuver block consisted of a stick rap, a doublet, and a frequency sweep in the pitch axis. Typical results of the real-time plot output are depicted in Fig. 7. Further details of the technique development can be found in Ref. 6. In addition to determining the FCS phase and gain margins, a real-time time history overlay of the actual aircraft flight response and predicted response was made from the same data. The predicted response was generated in real time by entering the control deflections measured in flight and the initial flight conditions into the mathematical models and calculating the predicted response. A typical example is shown in Fig. 8. Additional details of this method are contained in Ref. 7. This real-time comparison was an additional check on the FCS stability analysis in that it detected any aircraft stability degradation when clearing the aircraft to the next test point. An overall degradation in aircraft stability relative to predictions for any significant aircraft response was cause to slow or halt envelope expansion.

In-Flight Deflection Measurement

The FDMS was utilized for wing static structural divergence clearance; data were compared with aeroelastic wing deflection predictions. The data were also used in analysis programs designed to derive the estimated wing static divergence dynamic pressure. The entire system was located on the right-hand side of the aircraft, with the 12 LEDs on the upper right wing surface (Fig. 9). These LEDs were focused on two diode array receivers that were mounted in the right-hand side of the fuselage behind a 5- by 7-in glass window, just above the wingroot. One diode array focused on the inboard set of LEDs and the other on the outboard set. Typical results, obtained primarily in postflight data reduction, can be seen in Fig. 10. Real-time computation and display of the data were possible but not deemed necessary for envelope clearance. Wingbox twist data obtained from deflection measurements are plotted as a function of wing semispan. Chordwise and spanwise relative displacement of the LED targets yielded very reliable measurements of wing twisting and bending, respectively.

Structural Loads

The structural loads clearance of the X-29A aircraft was accomplished for both ACC and MCC wing modes primarily by postflight analysis. Structural load limit envelopes were developed for 80 percent and 100 percent of limit, based on the 80-percent design load ground proof test. These limits were monitored in real time on a color CRT presentation for the left canard, left lateral fuselage, left wing, and vertical tail loads. A typical real-time presentation is shown in Fig. 11. Exceeding any of these structural loads envelopes would have caused the pilot to break off a maneuver, halting any further envelope expansion to the next higher Mach number. Some results were used to modify any further maneuvering that might cause airframe loads to exceed their limits. This usually resulted in a real-time call to decrease or limit the normal load factor target condition of a given maneuver. For each airframe component, torque loads were compared with bending loads computed from in-flight strain gage measurements.

The canard actuator load limit was the only nonstructural load limit observed during real time. The monitoring of this limit was necessitated by the single-system hydraulic actuator capability. The limit was set at 80 percent of the actuator limit defined in terms of an equivalent load measured at the actuator. The common load factor expansion maneuvers, such as the constant-thrust pushover-pullup maneuver from 1-g stabilized flight and the constant-altitude windup turn, were used to obtain loads data.

Static wing divergence clearance was accomplished by use of both strain gage and FDMS data. Separate postflight analysis of the data with the Southwell technique[8] gave an estimate of the divergence speed, which was compared with predictions. The canard strain gage data were analyzed in a similar way to determine canard divergence

speed and were compared with predictions. The MCC wing mode allowed for temporarily fixed wing geometry during a constant-altitude windup turn, from which the loads data were generated. This mode allowed the pilot to manually set discrete 5° increments of flaperon from 5° trailing edge up to 25° (full) trailing edge down.

Remotely Augmented Vehicle

To assist in the collection of data of higher quality and larger quantity, the remotely augmented vehicle (RAV) system (Fig. 12) was incorporated into the X-29A aircraft. The pilot-assist version of the RAV system was tested in this phase. Aircraft state variables calculated from the telemetered data are input to the computers, which generate guidance and control information.

The RAV system has two operating modes. In the first mode, a ground-based computer drives a set of airborne guidance needles (Fig. 12(b)) through a radio uplink. The ground-based computer calculates the flightpath required to accomplish the maneuver and then computes error signals from the desired and actual values in the form of pitch, roll, and throttle position. These errors are telemetered to the vehicle and displayed as commands to the pilot using the instrument landing system needles and the speed bug as indicators. This guidance assists the pilot not only in flying maneuvers more precisely but also in the transition to new test points.

The maneuvers currently envisioned for this mode include (1) Mach number and altitude capture, (2) constant-angle-of-attack level turns, and (3) level accelerations and decelerations.

This system will be used during the research phase of the program. Past experiences with a RAV system on the HiMAT vehicle,[9] F-104,[10] and F-8 digital fly-by-wire aircraft[11] have proven the benefits of a more powerful ground-based computer in generating flight test maneuver guidance and control.

In the second mode of operation, the ground-based computers can command any surface on the aircraft to perform a series of time-dependent movements that are preprogrammed in both frequency and amplitude. For example, the canard may be commanded to go through a series of pulses, doublets, and sinusoidal frequency sweeps very similar to the longitudinal block in the ITB-1. This will allow the determination of control derivatives for each surface. Reference 12 contains further information on this RAV mode.

Concluding Remarks

The X-29A aircraft has a number of unique aspects that required a carefully planned and integrated flight test program to expand its 1-g and maneuver envelopes. The particular challenge was the multidiscipline approach on a single X-type airplane project. The integrated test block approach, coupled with real-time analysis for immediate aircraft clearance, was essential to the successful conclusion of the expansion phase. The X-29A program incorporated a number of new and innovative real-time display techniques to provide for safe and efficient envelope expansion. The use of real-time displays to provide for quick analysis of stability and control, dynamic and static structures, flight control systems, and other systems data greatly enhanced the productivity and safety of the flight test program.

References

[1]Sefic, Walter J., and Cutler, William, "X-29A Advanced Technology Demonstrator Program Overview," AIAA-86-9727, Apr. 1986.

[2]Hicks, John W., Kania, Jan, Pearce, Robert, and Mills, Glen, "Challenges in Modeling the X-29A Flight Test Performance," AIAA-87-0081, Jan. 1987.

[3]Moore, Archie L., "The Western Aeronautical Test Range of NASA Ames Research Center," NASA TM-85924, 1985.

[4]Kehoe, Michael W., "AFTI/F-16 Aeroservoelastic and Flutter Flight Test Program — Phase I," NASA TM-86027, 1985.

[5]"Military Specification — Flight Control Systems, Design, Installation, and Test of Piloted Aircraft, General Specification for," MILSPEC-F-9490D, June 1975.

[6]Bosworth, J.T., and West, J.C., "Real-time Open-Loop Frequency Response Analysis of Flight Test Data," AIAA-86-9738, Apr. 1986.

[7]Bauer, Jeffrey E., Crawford, David B., Gera, Joseph, and Andrisani, Dominick, "Real-Time Comparison of X-29A Flight Data and Simulation Data," AIAA-87-0344, Jan. 1987.

[8]Ricketts, Rodney H., and Doggett, Robert V., Jr., "Wind-Tunnel Experiments on Divergence of Forward-Swept Wings," NASA TP-1685, 1980.

[9]Duke, E.L., and Lux, D.P., "The Application and Results of a New Flight Test Technique," AIAA-83-2137, Aug. 1983.

[10]Meyer, R.R., Jr., and Schneider, Cdr. E.T., "Real-Time Pilot Guidance System for Improved Flight Test Maneuvers," AIAA-83-2747, Nov. 1983.

[11]Hartman, Gary, Stein, Gunther, and Powers, Bruce, "Flight Test Experience With an Adaptive Control System Using a Maximum Likelihood Parameter Estimation Technique," AIAA-79-1702, 1979.

[12]Shafer, Mary F., "Flight Investigation of Various Control Inputs Intended for Parameter Estimation," NASA TM-85901, 1984.

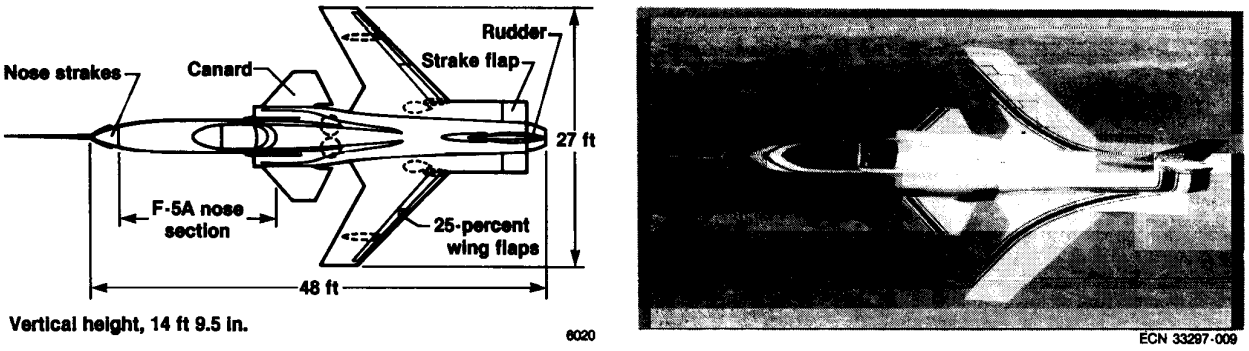

Fig. 1 X-29A advanced technology demonstrator.

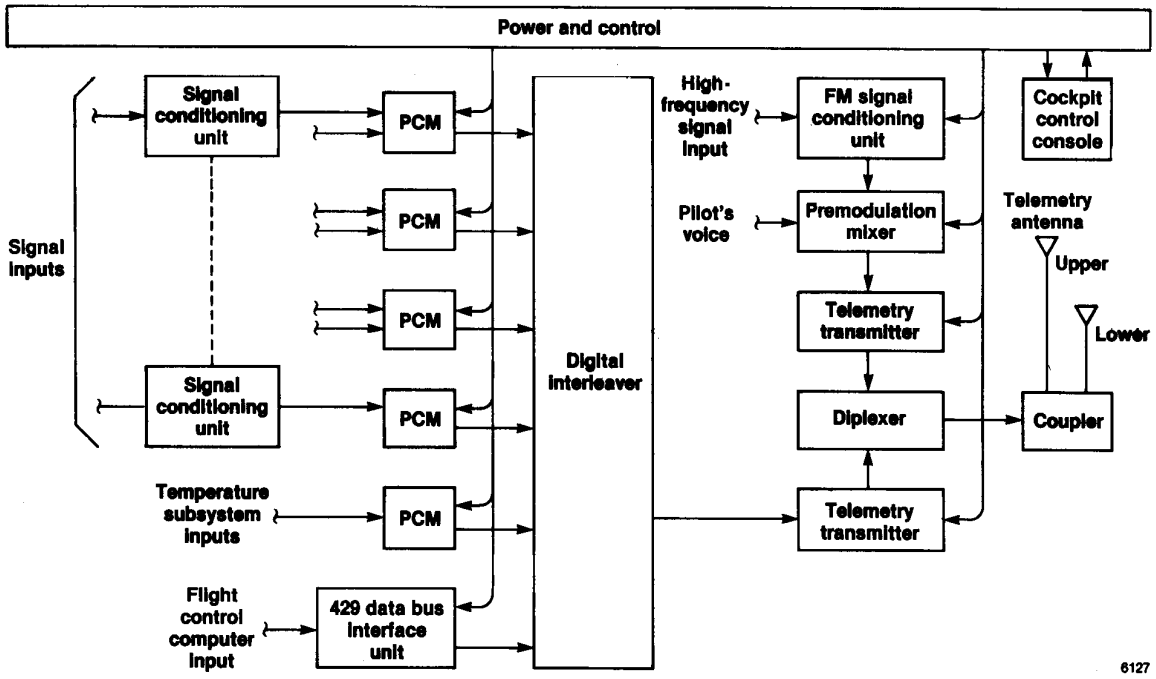

Fig. 2 X-29A data acquisition system.

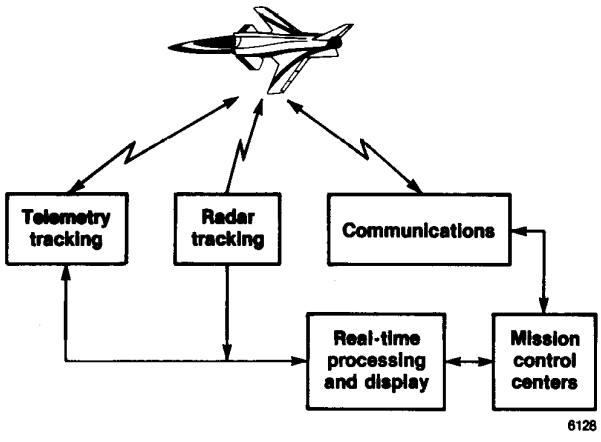

Fig. 3 Real-time processing and display.

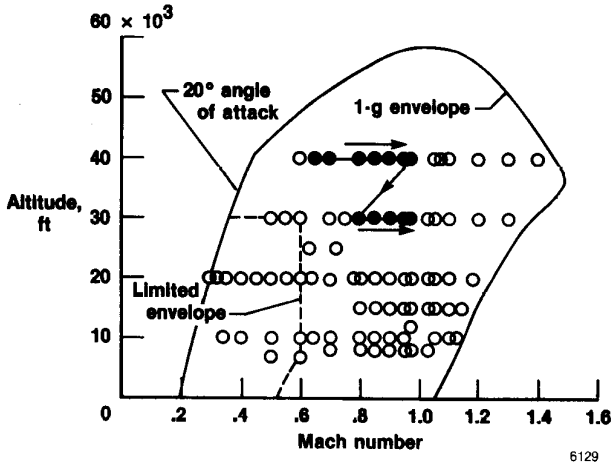

Fig. 4 Flight envelope expansion approach.

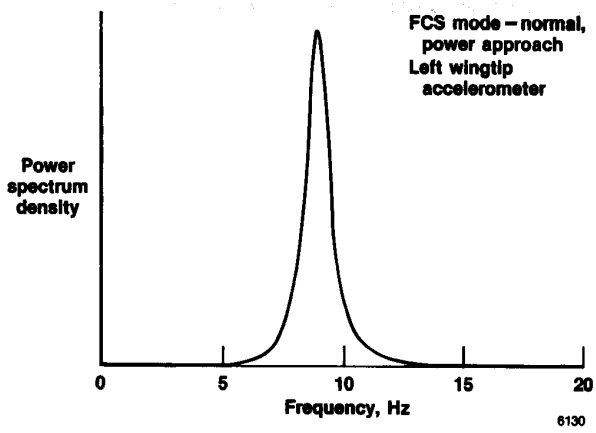

Fig. 5 Parabolic curve fit to determine frequency and damping in near real time.

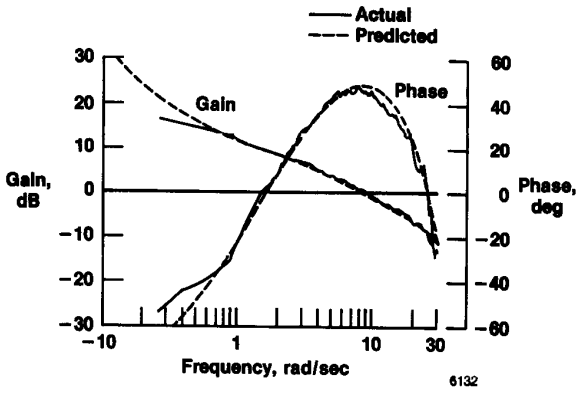

Fig. 7 Real-time FCS frequency response.

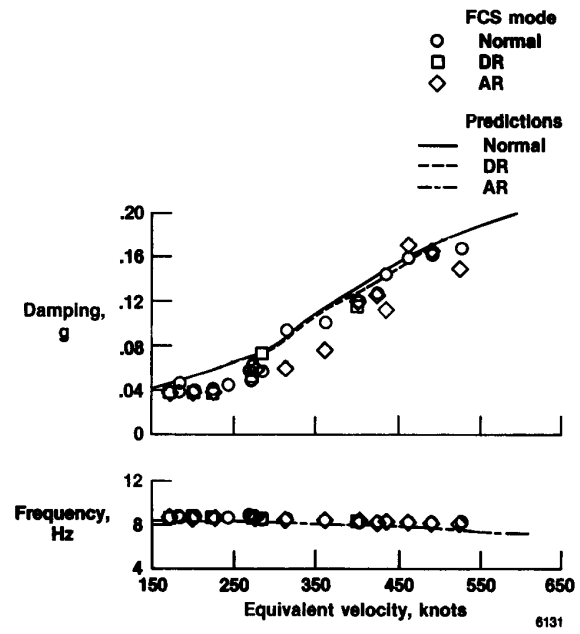

Fig. 6 Typical structural dynamics modal frequency and damping.

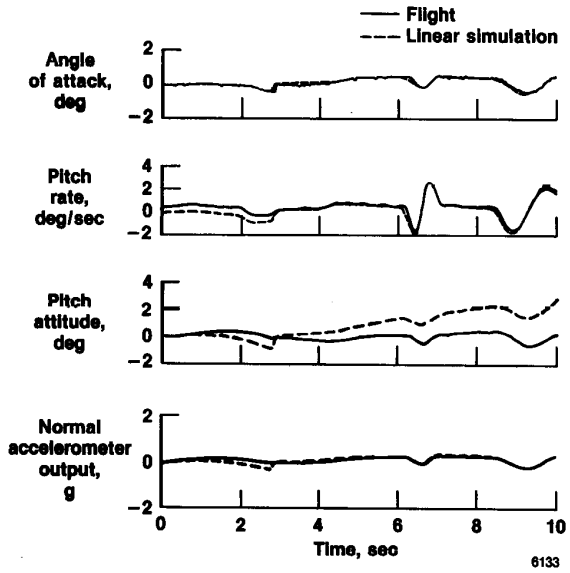

Fig. 8 Real-time computed longitudinal aircraft response.

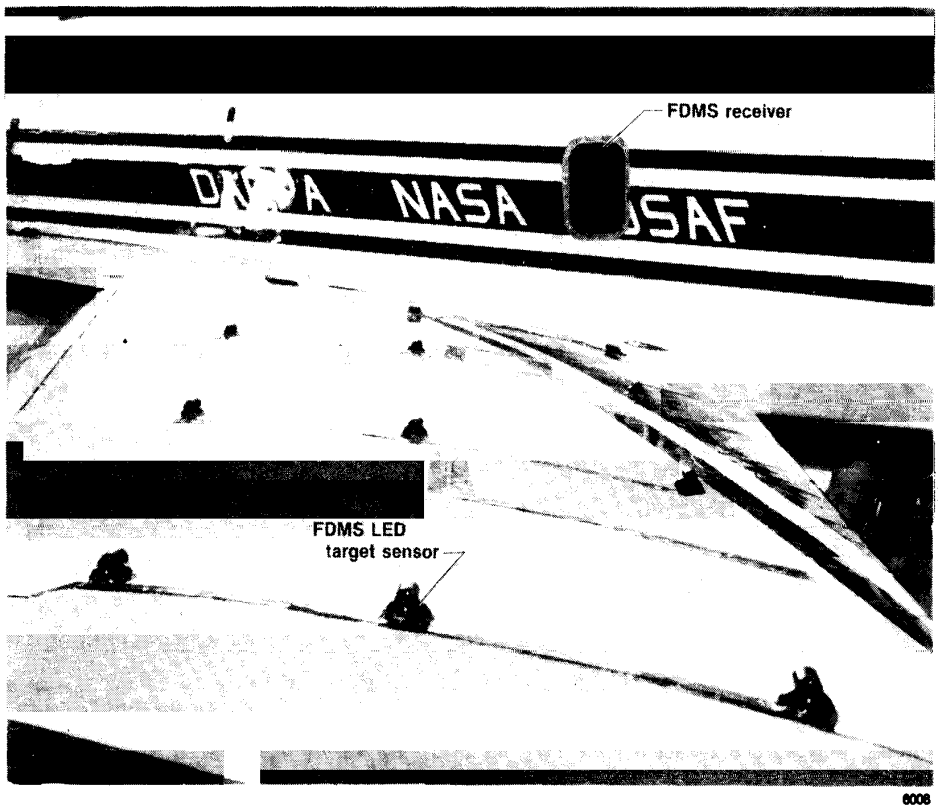

Fig. 9 Flight deflection measurement system.

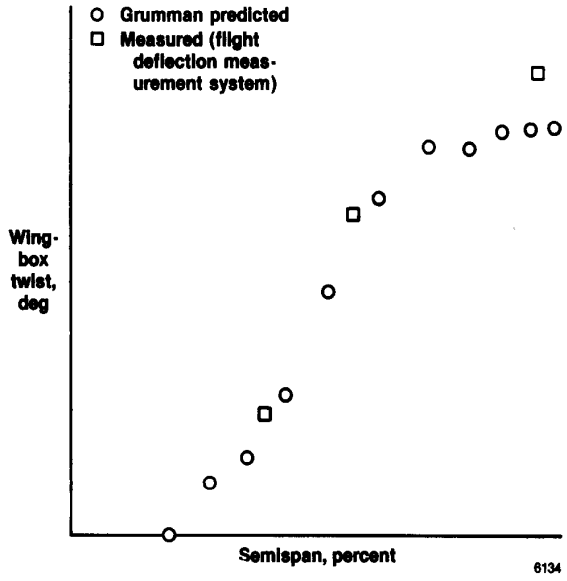

Fig. 10 Typical X-29A deflection measurement data for wingbox twist as a function of semispan compared with predicted data.

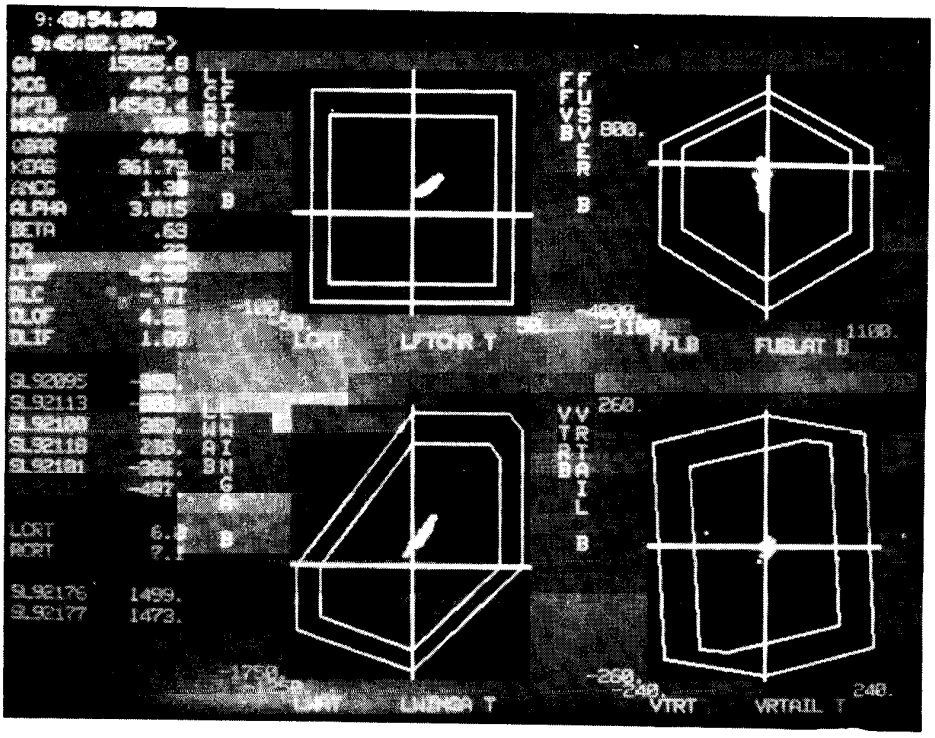

Fig. 11 Typical real-time graphics display of wing, canard, fuselage, and vertical tail bending as a function of torsion.

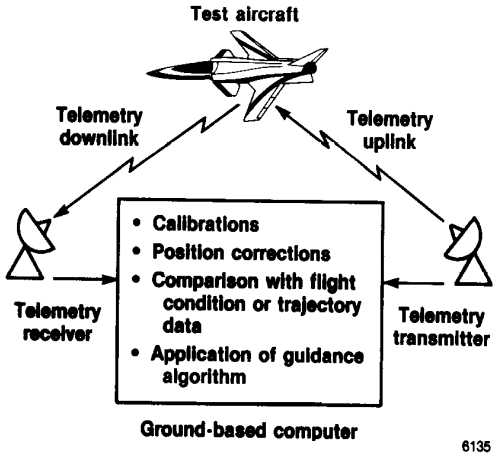

(a) Flight test trajectory guidance system.

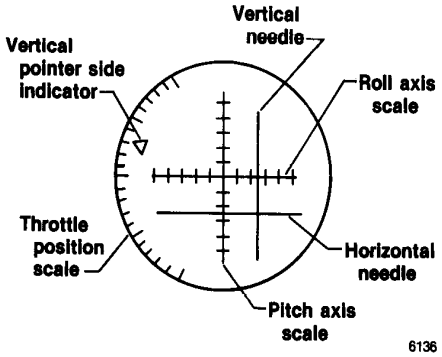

(b) Generic pilot display device.

Fig. 12 Remotely augmented vehicle system.

1. Report No.	2. Government Accession No.	3. Recipient's Catalog No.
NASA TM-88289		

4. Title and Subtitle	5. Report Date
FLIGHT TEST TECHNIQUES FOR THE X-29A AIRCRAFT	February 1987
	6. Performing Organization Code

7. Author(s)	8. Performing Organization Report No.
John W. Hicks, James M. Cooper, Jr., and Walter J. Sefic	H-1401
	10. Work Unit No. RTOP 533-02-51

9. Performing Organization Name and Address	11. Contract or Grant No.
NASA Ames Research Center Dryden Flight Research Facility P.O. Box 273 Edwards, CA 93523-5000	
	13. Type of Report and Period Covered: Technical Memorandum

12. Sponsoring Agency Name and Address	14. Sponsoring Agency Code
National Aeronautics and Space Administration Washington, DC 20546	

15. Supplementary Notes

Prepared as AIAA-87-0082 for presentation at the AIAA 25th Aerospace Sciences Meeting, Reno, Nevada, January 12-15, 1987.

16. Abstract

The X-29A advanced technology demonstrator is a single-seat, single-engine aircraft with a forward-swept wing. The aircraft incorporates many advanced technologies being considered for this country's next generation of aircraft. This unusual aircraft configuration, which had never been flown before, required a precise approach to flight envelope expansion. Special concerns were static wing divergence and a highly unstable airframe. Flight envelope expansion included the 1-g flight envelope and the maneuver envelope at higher normal load factors and angle of attack. Real-time analysis was required to clear the envelope in a safe, efficient manner. In some cases, this led to development of a unique real-time analysis capability. The use of real-time displays to provide for quick analysis of stability and control, dynamic and static structures, flight control systems, and other systems data greatly enhanced the productivity and safety of the flight test program.

This paper describes the real-time analysis methods and flight test techniques used during the envelope expansion of the X-29A aircraft, including new and innovative techniques that provided for a safe, efficient envelope expansion. The use of integrated test blocks in the expansion program and in the overall flight test approach will be discussed.

17. Key Words (Suggested by Author(s))	18. Distribution Statement
Flight envelope expansion Flight test techniques Forward-swept wing	Unclassified — Unlimited Subject category 05

19. Security Classif. (of this report)	20. Security Classif. (of this page)	21. No. of Pages	22. Price*
Unclassified	Unclassified	11	A02

*For sale by the National Technical Information Service, Springfield, Virginia 22161.